Synthesis of cuboid $PbZr_{0.52}Ti_{0.48}O_3$ nanocrystals by hydrothermal method

XINYI LI, JIUQIANG SONG, ZHIXIONG HUANG, DONGYUN GUO*
School of Materials Science and Engineering, Wuhan University of Technology, Wuhan 430070, China

$PbZr_{0.52}Ti_{0.48}O_3$ nanocrystals were prepared by a hydrothermal method using ammonia solution as a pH-adjusting agent. The $PbZr_{0.52}Ti_{0.48}O_3$ nanocrystals were analyzed by XRD, FESEM, TEM and PFM techniques. The single-crystal $PbZr_{0.52}Ti_{0.48}O_3$ nanocrystals with cuboid morphology were prepared by the hydrothermal method at 200 ^oC for 20 h. The existence of ferroelectric nanodomains confirmed that the cuboid $PbZr_{0.52}Ti_{0.48}O_3$ nanocrystals had ferroelectric properties.

(Received June 30, 2022; accepted December 5, 2022)

Keywords: Cuboid $PbZr_{0.52}Ti_{0.48}O_3$ nanocrystals, Hydrothermal method, Crystal structure, Ferroelectrics

1. Introduction

$PbZr_{0.52}Ti_{0.48}O_3$ compound with perovskite structure has been commercially applied in multilayer capacitors, piezoelectric transducers, pyroelectric detectors, energy harvesters, optical sensors and ferroelectric memories due to its excellent dielectric, ferroelectric and piezoelectric properties [1-2]. Due to the increasing need for miniaturization of electronic devices, nanoscale $PbZr_{0.52}Ti_{0.48}O_3$ compounds have been synthesized by various techniques, such as solid-state reaction, high energy ball-milling, sol-gel, wet chemical and hydrothermal methods, etc. [3-5]. Hydrothermal method has been widely applied in synthesis of $PbZr_{0.52}Ti_{0.48}O_3$ nanocrystals due to its simple equipment and low-energy consumption characteristics [5-10]. In the hydrothermal process, NaOH or KOH is usually used as a pH adjusting agent to synthesize $PbZr_{0.52}Ti_{0.48}O_3$ compounds. However, the undesirable alkali impurities are inevitably incorporated in the $PbZr_{0.52}Ti_{0.48}O_3$ crystal lattice. In the hydrothermal process, to resolve the contamination problem caused by alkali ions, $PbZr_{0.52}Ti_{0.48}O_3$ nanocrystals should be synthesized using an alkali-free pH adjusting agent. Cho et al. [7] firstly selected tetramethylammonium hydroxide (TMAH) as the pH-adjusting agent to synthesize micrometer-scale PZT particles by the hydrothermal method to avoid the contamination of alkalis. Recently, Takada et al. [8] investigated to synthesize micrometer-scale $Pb(Zr,Ti)O_3$ cubes by hydrothermal method with the pH-adjusting agent of TMAH. Since the strong corrosive and toxic TMAH agent is very expensive, it is necessary to find another alternative alkali-free pH-adjusting agent. In our previous study, the $PbTiO_3$ dendritic nanorods and nanosheets were synthesized by the hydrothermal method using ammonia solution as the pH-adjusting agent, which indicated that $PbZr_{0.52}Ti_{0.48}O_3$ nanocrystals could be synthesized using ammonia solution as the pH-adjusting agent [9, 10].

In this study, the cuboid $PbZr_{0.52}Ti_{0.48}O_3$ nanocrystals were synthesized by the hydrothermal method with ammonia solution as the pH-adjusting agent. The ferroelectric domains of cuboid $PbZr_{0.52}Ti_{0.48}O_3$ nanocrystals were analyzed via piezoresponse force microscopy (PFM) technique.

2. Experimental details

Lead acetate trihydrate ($Pb(CH_3COO)_2{\cdot}3H_2O$), bis(ammonium lactate) titanium dihydroxide ($C_6H_{18}N_2O_8Ti$), Zirconium n-propoxide ($C_{12}H_{28}O_4Zr$) were used as starting materials, and ammonia solution was used as the pH-adjusting agent. The desired amounts of $C_6H_{18}N_2O_8Ti$ and $C_{12}H_{28}O_4Zr$ were firstly dissolved in 10 ml ethanol at room temperature to form a Zr-Ti precursor. The ammonia solution was slowly added to the Zr-Ti precursor with stirring, and the nominal ammonia concentration in the Zr-Ti precursor was 6.6 mol/L. When a precipitate gel was formed, it was washed with ethanol and deionized water in sequence. Then, the precipitate gel and $Pb(CH_3COO)_2{\cdot}3H_2O$ were dispersed in deionized water to form a Pb-Zr-Ti precursor (30 ml) with nominal ammonia concentration of 6.6 mol/L. The 30 ml Pb-Zr-Ti precursor was added to a Teflon-lined autoclave of 50 ml capacity. The autoclave was sealed tightly, and heated at 200 ^oC for 20 h with continuous stirring. Finally, it was naturally cooled to room temperature. The precipitate was washed with deionized water and ethanol in sequence.

The crystal phase of the precipitate was analyzed by an X-ray diffractometer (XRD, D/MAX-RB) with Cu$K\alpha$ radiation (40 kV, 30 mA). Its morphologies were

characterized by a field emission scanning electron microscope (FESEM, JSM-7500F) and a high-resolution transmission electron microscope (HR-TEM, JEM-2100F). Energy-dispersive spectra (EDS) were examined on an ULTRA PLUS TEM equipped with EDS detector working at an accelerating voltage of 30 kV. The $PbZr_{0.52}Ti_{0.48}O_3$ nanocrystals were dispersed in ethanol to form a suspended solution, and the solution was dropped on a $Pt/Ti/SiO_2/Si$ substrate. The $PbZr_{0.52}Ti_{0.48}O_3$ nanocrystals were deposited on the $Pt/Ti/SiO_2/Si$ substrate, and heat-treated at 350 ^oC for 30 min to improve the interfacial contact between $PbZr_{0.52}Ti_{0.48}O_3$ nanocrystals and Pt coating for the ferroelectric domain measurement using the PFM (Nanoscope IV).

3. Results and discussion

Fig. 1 shows XRD result of the precipitate and its morphology. It was indexed to tetragonal $PbZr_{0.52}Ti_{0.48}O_3$ phase (JCPDS No. 33-0784). A series of sharp and clear diffraction peaks were observed, which were assigned to the tetragonal $PbZr_{0.52}Ti_{0.48}O_3$ phase. However, four weak diffraction peaks located at 26.4 ^{o}, 27.0^o, 34.1^o and 36.0^o were also observed, which indicated that the impurity phase ($H_2Ti_3O_7$) co-existed with $PbZr_{0.52}Ti_{0.48}O_3$ phase. The inset in Fig. 1 shows the typical morphology of $PbZr_{0.52}Ti_{0.48}O_3$ precipitate. The rectangular and square grains were observed, which was mainly due to the observation of the cuboid $PbZr_{0.52}Ti_{0.48}O_3$ nanocrystals from different angles as shown in the schematic inset.

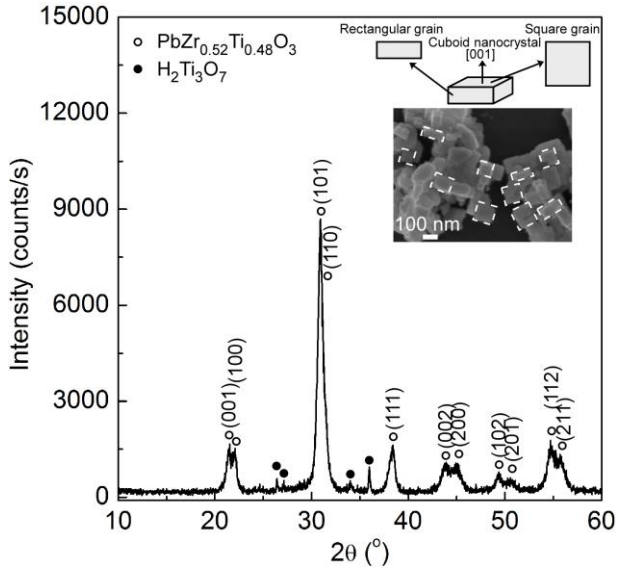

Fig. 1. XRD pattern of the precipitate and the inset shows its morphology

Fig. 2 displays the TEM image and selected area electron diffraction (SAED) pattern of the $PbZr_{0.52}Ti_{0.48}O_3$ nanocrystal. A typical cuboid $PbZr_{0.52}Ti_{0.48}O_3$ nanocrystal was observed, and the lateral size was about 90 nm, as shown in Fig. 2(a). The inset of Fig. 2(a) shows the corresponding SAED pattern. Its normal axis corresponded to the *c*-axis. The measured angles between (100) plane and (010) plane, (100) plane and (110) plane were 90.1^o and 45.2^o, respectively. According to the tetragonal $PbZr_{0.52}Ti_{0.48}O_3$ phase (JCPDS 33-0784), the calculated angles between (100) plane and (010) plane, (100) plane and (110) plane were 90^o and 45^o, respectively. The values of measured angles were very close to those of calculated angles. The high-resolution TEM image of the encircled area in Fig. 2(a) is shown in Fig. 2(b). The lattice fringes with interplanar distances of 0.3965 and 0.4000 nm were indexed as (010) and (100) planes of tetragonal $PbZr_{0.52}Ti_{0.48}O_3$ phase, respectively. Fig. 3 shows the high-angle annular dark field (HAADF) scanning TEM image, and elemental mapping images using EDS analysis of the cuboid $PbZr_{0.52}Ti_{0.48}O_3$ nanocrystal. The Pb, Zr, Ti and O ions were homogeneously distributed within the cuboid $PbZr_{0.52}Ti_{0.48}O_3$ nanocrystal. The chemical composition of the cuboid $PbZr_{0.52}Ti_{0.48}O_3$ nanocrystal was calculated, and the normalized molar ratio of Pb:Zr:Ti was 1:0.53:0.49, which was close to the stoichiometric molar ratio of $PbZr_{0.52}Ti_{0.48}O_3$. These results confirmed that the single-crystal $PbZr_{0.52}Ti_{0.48}O_3$ nanocrystal was synthesized.

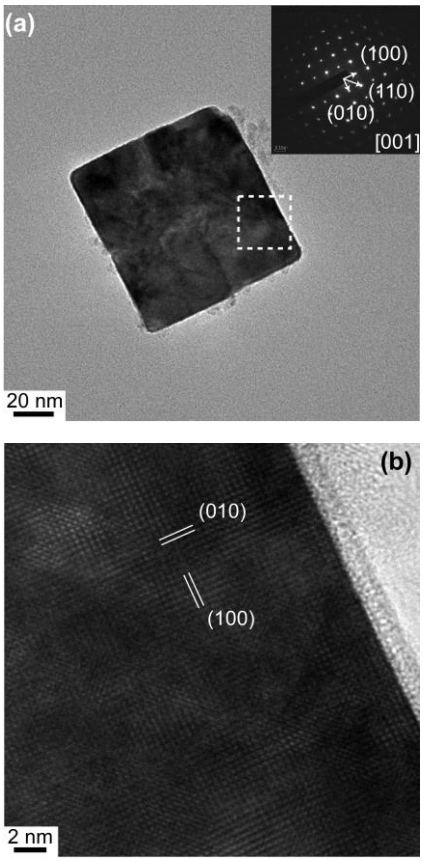

Fig. 2. TEM image (a) of cuboid $PbZr_{0.52}Ti_{0.48}O_3$ nanocrystal, the inset shows its corresponding SAED pattern, and high-resolution TEM image (b) of the selected area encircled by dashed line in (a)

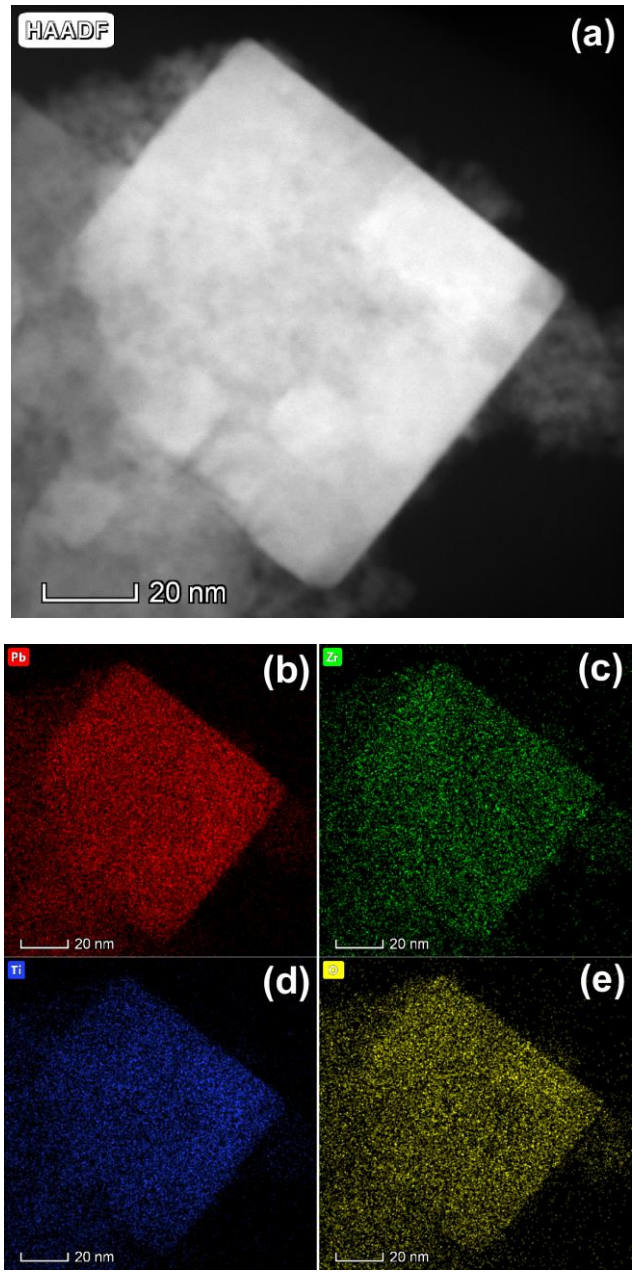

Fig. 3. (a) HAADF STEM image of cuboid $PbZr_{0.52}Ti_{0.48}O_3$ nanocrystal, and elemental mapping images using EDS analysis corresponding to the cuboid $PbZr_{0.52}Ti_{0.48}O_3$ nanocrystal: (b) Pb, (c) Zr, (d) Ti and (e) O (color online)

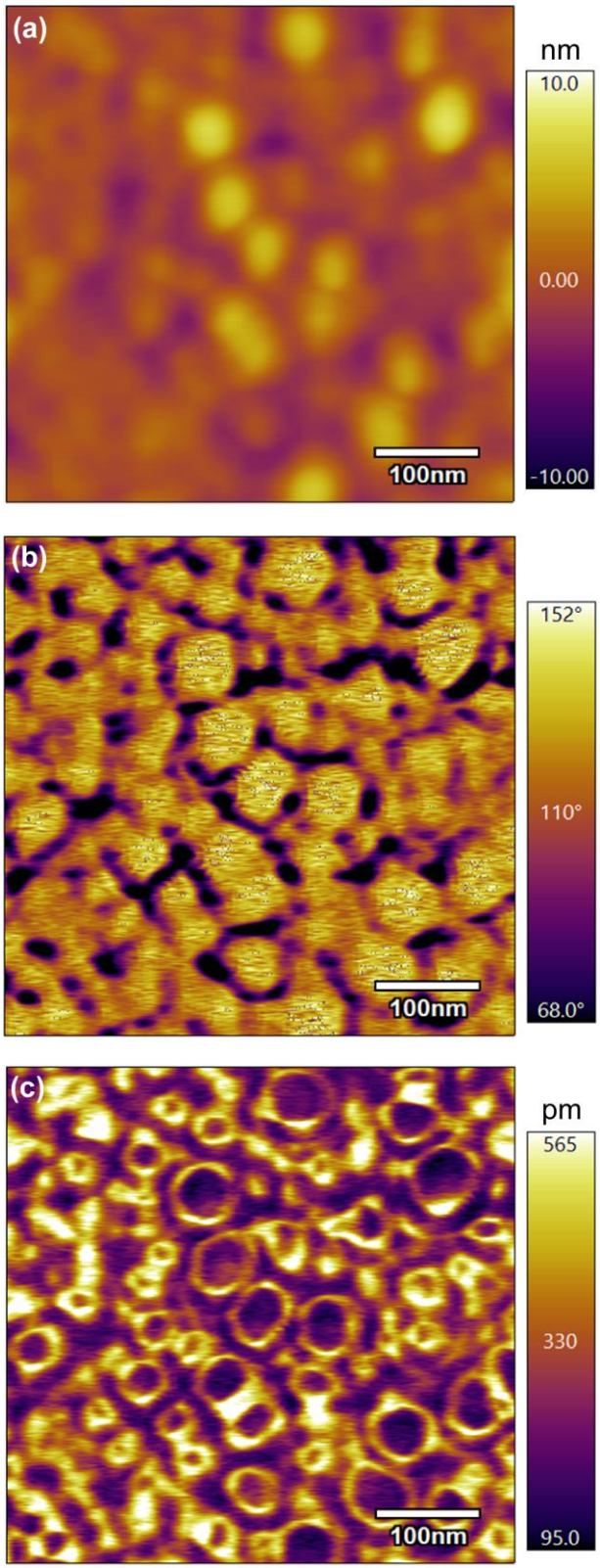

Fig. 4. Topography (a), PFM phase (b) and amplitude (c) for the same region of $PbZr_{0.52}Ti_{0.48}O_3$ nanocrystals deposited on Pt/Ti/SiO_2/Si substrate (color online)

For the PFM measurement, a voltage (5 V, peak-to-peatk at 40 Hz) was applied to a metal-coated tip. Fig. 4 displays the PFM topography, vertical phase and amplitude results of the $PbZr_{0.52}Ti_{0.48}O_3$ nanocrystals deposited on $Pt/Ti/SiO_2/Si$ substrate. The PFM amplitude signal was proportional to the local piezoelectric coefficient of the ferroelectric domain along the out-of-plane direction. The out-of-plane polarization direction was indicated in the PFM phase by bright yellow, dark and noisy regions, which represented domain up, down and no PFM response, respectively [11]. According to Figs. 4(b) and (c), the PFM response varied weakly as a function of position within a single $PbZr_{0.52}Ti_{0.48}O_3$ nanocrystal, which indicated that ferroelectric nanodomains had the same dimension as the $PbZr_{0.52}Ti_{0.48}O_3$ nanocrystals.

4. Conclusion

The single-crystal $PbZr_{0.52}Ti_{0.48}O_3$ nanocrystals were obtained by the hydrothermal method at 200 ^oC for 20 h using ammonia solution as the pH-adjusting agent, and the $PbZr_{0.52}Ti_{0.48}O_3$ nanocrystals had cuboid morphology. The existence of ferroelectric nanodomains confirmed that the cuboid $PbZr_{0.52}Ti_{0.48}O_3$ nanocrystals had ferroelectric properties. In the next research, further investigation should be done to obtain the single-phase cuboid $PbZr_{0.52}Ti_{0.48}O_3$ nanocrystals.

Acknowledgement

This work was supported by the National Natural Science Foundation of China (Grant No. 51272195).

Financial interests

The authors declare they have no financial interests.

References

[1] G. Tan, K. Maruyama, Y. Kanamitsu, S. Nishioka, T. Ozaki, T. Umegaki, H. Hida, I. Kanno, Sci. Rep. **9**, 7309 (2019).
[2] J. F. Scott, Science **315**, 954 (2007).
[3] T. Yamada, D. Ito, T. Sluka, O. Skata, H. Tanaka, H. Funakubo, T. Namazu, N. Wakiya, M. Yoshino, T. Nagasaki, N. Setter, Sci. Rep. **7**, 5236 (2017).
[4] Q. Wan, Q. Gu, J. Xing, J. Chen, Mater. Lett. **92**, 52 (2013).
[5] X. Li, Q. Ma, Z. Huang, L. Zhang, D. Guo, Y. Ju, J. Mater. Sci.-Mater. Electron. **30**, 17164 (2019).
[6] C. Glass, W. Ahmed, J. van Ruitenbeek, Mater. Lett. **125**, 71 (2014).
[7] S. Cho, M. Oledzka, R. E. Riman, J. Cryst. Growth **226**, 313 (2001).
[8] Y. Takada, K. Mimura, Z. Liu, K. Kato, J. Cryst. Growth **548**, 125811 (2020).
[9] X. Li, Z. Huang, L. Zhang, D. Guo, Electron. Mater. Lett. **14**, 610 (2018).
[10] J. Yue, Z. Huang, D. Guo, Y. Ju, Optoelectron. Adv. Mat. **15**(9-10), 504 (2021).
[11] A. L. Kholkin, I. K. Bdikin, D. A. Kiselev, V. V. Shvartsman, S. H. Kim, J. Electroceram. **19**, 81 (2007).

*Corresponding author: guody@whut.edu.cn